JOURNAL OF CHEMOMETRICS
J. Chemometrics 2003; **17**: 200–215
Published online in Wiley InterScience (www.interscience.wiley.com). DOI: 10.1002/cem.790

Review

Practical aspects of PARAFAC modeling of fluorescence excitation-emission data

C. M. Andersen[1,2]* and R. Bro[1]

[1]The Royal Veterinary and Agricultural University, Department of Food Science, Food Technology, Rolighedsvej 30, DK-1958 Frederiksberg C, Denmark
[2]Danish Institute for Fisheries Research, Department of Seafood Research, DTU Building 221, DK-2800 Kgs. Lyngby, Denmark

Received 1 November 2002; Revised 24 January 2003; Accepted 27 January 2003

This paper presents a dedicated investigation and practical description of how to apply PARAFAC modeling to complicated fluorescence excitation–emission measurements. The steps involved in finding the optimal PARAFAC model are described in detail based on the characteristics of fluorescence data. These steps include choosing the right number of components, handling problems with missing values and scatter, detecting variables influenced by noise and identifying outliers. Various validation methods are applied in order to ensure that the optimal model has been found and several common data-specific problems and their solutions are explained. Finally, interpretations of the specific models are given. The paper can be used as a tutorial for investigating fluorescence landscapes with multi-way analysis. Copyright © 2003 John Wiley & Sons, Ltd.

KEYWORDS: validation; scatter; missing values; outliers

1. INTRODUCTION

Fluorescence spectroscopy has been used in many scientific fields, such as chemistry, medicine, environmental and food science. However, fluorescence signals can be rather complex and, therefore, the analysis might become complicated owing to interferences, scatter, overlapping signals, etc.

When autofluorescence of every sample is measured at several emission wavelengths for several excitation wavelengths, the interpretation can be facilitated by the use of multi-way models such as PARAFAC [1], Tucker and N-PLS [2–4]. If the data are approximately trilinear, curve resolution is possible by the use of PARAFAC, possibly providing estimates of the spectra and concentration profiles of the underlying chemical analytes, thus relating the measured autofluorescence of mixtures to chemical knowledge about the material [2,5]. When modeling fluorescence data, interference from scattered light (primarily Rayleigh and Raman scattering) can give a slight model inadequacy influencing the estimated model parameters. Furthermore, other factors such as quenching and instrumental noise can cause problems. Therefore, consideration of the various influential contributions is important when analyzing fluorescence excitation–emission data and when interpreting the derived models.

Several studies have explored and described the underlying chemical phenomena in fluorescence spectral data by applying multi-way modeling such as PARAFAC. For example, Ross *et al.* [6] described the underlying structure of fluorescence spectra obtained from pigment complexes in pea thylakoids. In other studies, PARAFAC models based on fluorescence landscapes of sugar solutions were used to obtain information regarding both sugar quality and process parameters [7,8]. It was shown that tryptophan and tyrosine and also high molecular weight Maillard reaction polymers and polyphenolic compounds were important fluorophores. In an investigation of the interactions between a non-fluorescent DDT-type pesticide and a fluorescent dye, PARAFAC was employed to find the fluorescence profiles of complexed dye states [9]. Furthermore, the ability to quantify trace pesticides and polycyclic aromatic hydrocarbons by fluorescence spectroscopy and PARAFAC modeling was investigated by Jiji *et al.* [10]. They showed the possibility of resolving the analyte spectra from overlapping fluorescence signals, scatter and instrumental background. PARAFAC was also applied to describe and predict the amount of dissolved chlorophyll and pheophytin pigments [11]. Dioxin contents of fish oils were estimated

*Correspondence to: C. M. Andersen, The Royal Veterinary and Agricultural University, Department of Food Science, Food Technology, Rolighedsvej 30, DK-1958 Frederiksberg C, Denmark.
E-mail: cma@kvl.dk
Contract/grant sponsor: LMC (Center for Advanced Food Studies).
Contract/grant sponsor: AQM (Advanced Quality Monitoring).
Contract/grant sponsor: Ministries of Research and Industry.
Contract/grant sponsor: EU; Contract/grant number: GRD1-10337, NWAYQUAL.

by PARAFAC modeling of fluorescence landscapes [12]. It was suggested that the relations obtained were due to quenching effects or other complex chemical factors in the fish oils.

There are several publications describing the theory and giving examples of PARAFAC modeling [1,3,4,13,14]. Furthermore, the applications given above illustrate the advantages of using PARAFAC for analyzing fluorescence spectroscopic data and show how PARAFAC can be applied to interpret such data. However, no articles have discussed in depth the practical aspects of using PARAFAC for decomposing fluorescence excitation–emission matrices (EEMs). Important practical issues such as how to determine the optimal number of components, how to handle disturbing scatter signals and how to deal with missing values, find outliers and validate the model are mostly just described superficially.

This paper demonstrates in detail how the use of a suitable mathematical model such as PARAFAC can help understanding the underlying spectral and chemical phenomena in a complex system. In particular it provides guidelines and tools for the proper handling of many of the typical problems that arise in the modeling of fluorescence excitation–emission data. Hence the paper can be used as a tutorial for investigating fluorescence landscapes with multi-way analysis. Measurements on fish muscle extracts are used as an example and illustrate the possibility of using fluorescence spectroscopy for on-line quality monitoring in the fish industry. Additionally, fluorescence excitation–emission matrices of solutions with known concentrations of four fluorophores are analyzed. Including both data sets in the presentation provides an illustration of how both well-characterized (and well-behaved) data and less well-characterized data can be analyzed.

2. MATERIALS AND METHODS

2.1. Fish data

A factorial design with two frozen storage temperatures (−20 °C and −30 °C), four frozen storage periods (3, 6, 9 or 12 months) and five chill storage periods (0, 3, 7, 14 or 21 days at 2 °C) was used. Cod (*Gadus morhua*) from a single catch were caught in February 1999 in the Barents Sea. Experiments after 3 months of frozen storage at −20 °C were left out for practical reasons, giving a total of 35 storage conditions. The chill storage was made in modified atmosphere (40% CO_2/40% N_2/20% O_2). Three packs with each storage treatment were analyzed, giving a total of 105 samples.

Aqueous extracts were made by homogenizing 25 g of fish muscle with 75 ml of water. The pH was reduced to 5.2 with 2 M HCl and the mixture was heated to 70 °C, cooled to room temperature and filtered to remove precipitated proteins. This treatment provides a clear solution containing a number of fluorophores but of lower chemical complexity than if the raw fish muscles were measured. The extracts were stored at −30 °C.

The extracts were measured spectrofluorimetrically at 22 °C in a 10 × 10 mm thermostated quartz cuvette on a Perkin-Elmer LS50B spectrofluorimeter. Raw non-smoothed data were recorded. For every sample, an excitation–emission matrix (EEM) was obtained by measuring the emission spectra from 270 to 600 nm at 2 nm intervals with excitation at every 10 nm from 250 to 370 nm. These wavelengths were chosen from a preliminary experiment based on which areas showed the highest variability (not shown). The measurements started with the highest excitation wavelength and ended with the lowest in order to minimize photodecomposition of the sample [15]. Based on the visual appearance of the preliminary experiments, the excitation and emission slit widths were both set to 7 nm and the scan speed was 750 nm s^{-1}.

All measurements were made within a few days to minimize the effect of instrumental drift and changes in lamp intensity. Such changes could have required suitable standardization [16]. A solution of 15 g of ordinary white sugar per 100 ml of doubly deionized water was used as a standard and measured three times a day to verify that instrumental changes did not influence the results [16]. No substantial variations among the sugar samples were found. The fish muscle extracts were measured in random order.

2.2. Data with known fluorophores

This data set contains fluorescence landscapes of 27 samples containing different concentrations of four fluorophores with fairly similar spectral properties [17]. The four compounds are phenylanaline, 3,4-dihydroxyphenylalanine (DOPA), 1,4-dihydroxybenzene and tryptophan.

The measurements were performed on the same Perkin-Elmer LS50 B fluorescence spectrometer as the fish data with excitation wavelengths ranging between 200 and 315 nm (5 nm intervals) and emission wavelengths ranging from 250 to 459 nm (1 nm intervals). Both the excitation and emission slit widths were set to 5 nm and the scan speed was 1500 nm min^{-1}.

2.3. Multi-way data analysis

Ideally, the data arranged in an $I \times J \times K$ three-way array will be trilinear [2]. The first index (I) refers to the samples, the second (J) to the emission wavelengths and the third (K) to the excitation wavelengths (Figure 1).

PARAFAC [1,13] was used to model the data. The PARAFAC model can be written as

$$x_{ijk} = \sum_{f=1}^{F} a_{if} b_{jf} c_{kf} + e_{ijk}$$
$$i = 1, \ldots, I;\ j = 1, \ldots, J;\ k = 1, \ldots, K$$

where x_{ijk} is the intensity of the ith sample at the jth variable (emission mode) and at the kth variable (excitation mode) a_{if}, b_{jf} and c_{kf} are parameters describing the importance of the samples/variables to each component and the residuals, e_{ijk}, contain the variation not captured by the model.

The PARAFAC components will be estimates of the signals from the individual fluorophores if the data are approximately low-rank trilinear and when the correct number of components is used. In that case, the scores in a_{if} may be interpreted as the relative concentration of analyte f in sample i. The J-vector $\mathbf{b}_f$ with elements b_{jf} (j = 1, …, J) is the estimated emission spectrum of this analyte and likewise $\mathbf{c}_f$ is the estimated excitation spectrum. In order for the

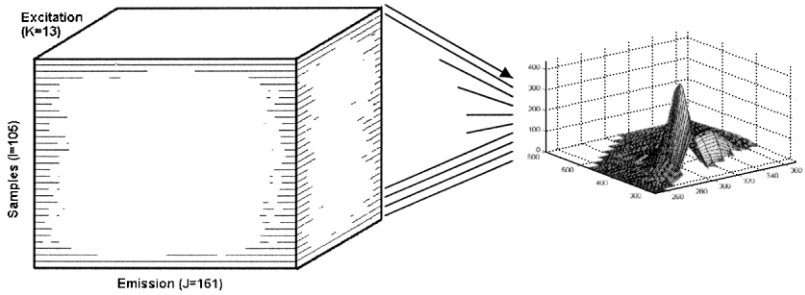

Figure 1. Arrangement of the data in a three-way structure.

decomposition to be unique and provide meaningful estimates, some mathematical conditions must be fulfilled. For example, no two spectra may be identical. In fact, if all spectra and concentration profiles are linearly independent, the decomposition is unique. More relaxed conditions can also be given [18]. The model states that for each analyte, the contribution to the measured excitation–emission matrix is $a_{if}\mathbf{b}_f\mathbf{c}_f^{\mathrm{T}}$, which is the landscape of a pure analyte scaled by the concentration. This reflects that additivity and linearity of the signal is assumed to be valid. A change in concentration only changes the magnitude of the contribution (a_{if}) not the actual shape ($\mathbf{b}_f\mathbf{c}_f^{\mathrm{T}}$). Both concentrations and spectra are only determined up to a scaling because, e.g., the vector $\mathbf{b}_f$ may be exchanged with $1/2\mathbf{b}_f$ as long as, for example, $\mathbf{c}_f$ is exchanged with $2\mathbf{c}_f$. Such a change will not change the contribution to the model ($a_{if}\mathbf{b}_f\mathbf{c}_f^{\mathrm{T}} = a_{if}1/2\mathbf{b}_f2\mathbf{c}_f^{\mathrm{T}}$).

Inner-filter effects caused by high concentrations, scattering and quenching can disturb the trilinearity of the data. Furthermore, abundance of missing data (see later) and spectral similarities can lead to uncertain estimates. Therefore, the chemical interpretation should be exercised with care. In the following it is shown how a PARAFAC model can be validated using fit values, visual assessment of the loadings, residual analysis, core consistency diagnostic, jackknifing and by a split-half analysis [19].

For further in-depth descriptions of PARAFAC theory and algorithms we refer to other publications [1,2,4,5,13,14]. All analyses were performed with the N-way toolbox (www.models.kvl.dk) and Matlab version 5.3 (The MathWorks, Natick, MA, USA).

2.4. Data pretreatment

For the fish data set, emissions from 270 to 280 nm were removed from the data to reduce the amount of Rayleigh scatter and missing values. This gives a three-way array of the size $105 \times 161 \times 13$. For the data set with the four known fluorophores, the size of the array is $27 \times 210 \times 24$.

There is no emission below the excitation wavelength as this would correspond to higher energy being emitted than the energy causing the emission. Therefore, below the excitation wavelength, the emission is zero (or some noise equivalent to zero), regardless of the chemistry. Hence, for a complete EEM landscape a triangular part will be trivially zero, which has to be respected by the subsequent model. These zero values do not conform to the trilinear model, which is valid for the remaining part of the data. If this is not respected, misleading results can be obtained. The most common way to handle this problem is to set these values to missing in the analysis.

It is worth considering in more detail why emission below excitation cannot generally be simply set to or kept at zero in PARAFAC modeling. Emission wavelengths below the excitation wavelength do not exhibit any fluorescence and the measured intensity is therefore zero up to noise. However, part of an estimated excitation spectrum may have non-zero values at wavelengths higher than the corresponding estimated emission spectrum. An example of this is given for tyrosine in Figure 2 (top part). The PARAFAC model of a measured excitation–emission landscape is found as the outer product of the estimated excitation and emission spectrum. Hence, for emission below excitation, the model will have non-zero values as shown for tyrosine. However, this is physically impossible in practice. No fluorescence will occur and only zero signal (plus possible scatter) will be measured. Hence the trilinear PARAFAC model will not be valid for this part.

The middle-left plot in Figure 2 shows that similar spectra are obtained for different excitation wavelengths when the model of the data is set to missing for emission below excitation. The plot also shows that a one-component bilinear model can model the data adequately because all spectra have the same shape regardless of excitation. The relevant parts of the plot are shown in detail in the bottom-left part of Figure 2 (indicated by a circle in the middle plot). When the emission is set to zero as in the middle-right plot, an interesting phenomenon appears. Every emission spectrum is now different in shape because the zeros appear at different places for different excitations. Clearly, such a data set cannot be modeled by a single bilinear component as is the model in PARAFAC. In fact, many components are needed in order to handle the fact that every emission spectrum is different. This is contradictory to the underlying assumptions and hence the incorporation of zeros hinders adequate analysis of data.

In the above example, the problematic area is only the emission wavelengths slightly below the excitation wavelengths. The problem is that the chemical model, which is only valid for emission above excitation, is extended below for mathematical reasons. Emissions *far* below the excitation wavelength, however, are mostly zero both physically and mathematically. Hence in these areas it is less problematic to introduce zeros. However, other problems than the above-mentioned can cause zeros to be invalid. For example, for a double-fluorophoric molecule, a double peak might occur in

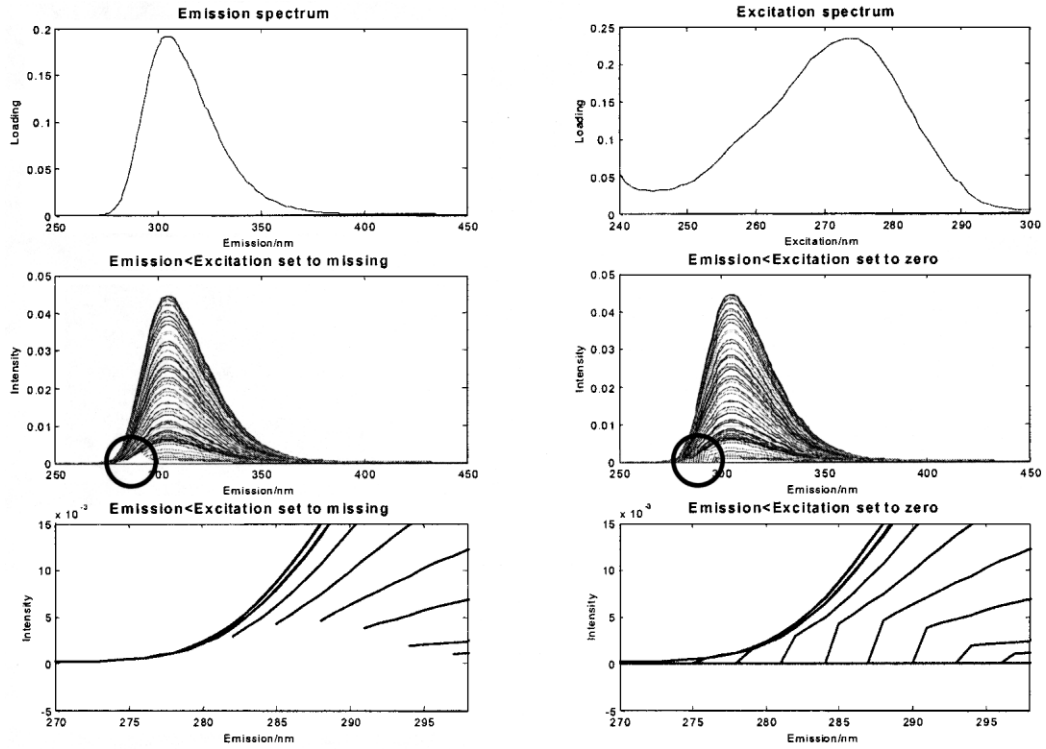

Figure 2. Illustration of the inadequate use of PARAFAC for fluorescence emission below the excitation wavelength. Top plots show the emission and excitation spectrum of tyrosine. The left middle plots show the emission spectra measured at several excitation wavelengths with emission below excitation set to missing. A smaller fraction indicated by the circle is shown blown up below. The right middle and bottom plots show the same but with emission below excitation set to zero. As can be seen at bottom-right, a rank-one approximation is not valid when zeros are present because the different emission spectra no longer have the same shape owing to the incorporated zeros.

both the excitation and the emission spectra of the molecule and this can lead to ghost peaks in the emission below excitation area. These will then be incorrectly forced to zero if zeros are maintained in this area. Before discussing the possible ways to handle emission below excitation, another problematic feature of EEM data is described.

Scattering (or reflection) is brought about by small particles in the samples, and causes the light to deviate from its original path and spread in all directions. The scattering does not contain any information on the fluorescence properties of the sample. Even non-fluorescent samples give rise to several peaks in a fluorescence spectrum. These peaks arise from elastic Rayleigh scatter, inelastic Raman scatter and complex, but predictable, harmonic order reflections of these same scatter peaks caused by the diffraction grating employed in the monochromator of the instrument (zeroth, first, etc., order scattering). In fluorescence EEMs, the scatter effects show up as diagonal lines across the landscapes. For elastic scattering there is no energy loss, so the scattered emission wavelength is identical with that of the exciting light. For inelastic scattering there is an energy loss associated with the scattering light, i.e. the scattered emission is shifted to longer wavelengths compared with the incident light. Both the Rayleigh and Raman scattering intensities will vary with solvent type and the quantity of dissolved particles in solution but Rayleigh scatter is often the most troublesome to handle [15]. Owing to Rayleigh scatter, emission in a window around the excitation wavelength does not conform to a trilinear model or, rather, the emission above the excitation has a contribution from the trilinear fluorescence signal as well as from the non-trilinear scatter signal.

There are several ways to deal with the non-chemical areas (the zeros and the scatter). In this case, the emission measurements up to slightly above the excitations are simply set to missing. Emissions obtained at the wavelengths around twice the excitation wavelength will be influenced by second-order Rayleigh scatter and are also replaced with missing values. The algorithms used to handle the missing data were described by Bro [4]. In the literature, other approaches have also been adopted [14,20–24], such as using zeros or down-weighting elements where emission is lower than excitation. The purposes of using these alternatives are basically the same (minimize the influence of non-trilinear parts) and no systematic investigations have yet been made to compare them. The current experience is that as long as the influence of the most significant Rayleigh scatter containing parts is minimized, the results are often similar.

3. RESULTS AND DISCUSSION

The steps and problems involved in finding a valid PARAFAC model for describing fluorescence excitation–emission data are given below. The appropriate number of

components is determined based on several different criteria. For example, the visual appearance of the loadings is a useful diagnostic because fluorescence spectra of liquids are typically characterized by broad and often unimodal peaks. Furthermore, the variance explained by the model, the number of iterations and the so-called core consistency diagnostic [4] are used. An important discussion on the influence of scatter and missing values is included in the following. How to correct for possible artifacts from these by constraining the model is described next. Only the determination of the number of components for the fish data set is illustrated in detail, since the procedure is similar for the other data set. An evaluation of the reliability of the score values by a jack-knife based approach is used together with the leverage and the distribution of sample residuals for identifying outlying samples. After removing grossly disturbing outliers, the models are validated by a split-half analysis. All diagnostic tools used to assess the models have pitfalls and only by using several quantitative and qualitative tools can a thorough conclusion be reached.

3.1. Building the PARAFAC model

3.1.1. Fish data

3.1.1.1. Initial PARAFAC modeling. Unconstrained PARAFAC models are calculated using from one to five components. It is expected that a two-component model is optimal since the fluorescence landscapes contain two visually recognizable peaks (Figure 3). However, peaks of fluorophores with a low quantum yield or low concentration may not be seen because of the dominant response of other fluorophores. This is especially so when their excitation and emission maxima are in the same wavelength areas as the dominant ones. Therefore, it is possible that more than two fluorophores contribute to the fluorescence spectra obtained here.

The explained variance indicates that three components are optimal because the increase obtained with more than three components is small relative to the increase in explained variance obtained using up to three components (Table I). Additionally, the percentage of variance explained using three components is adequate for this type of data. This is known from experience but can also be quantitatively evaluated based on the pooled standard deviation of replicate measurements, which is found to vary between 0.9 and 9.3. Comparing this with the pooled residuals of the three-component model of 4.3 and 6.5 for the two-component model shows that, for both the two-component and the three-component models, the amount of unmodeled variation in the data agrees with the variation between replicates and therefore the un-modeled part of the data can largely be attributed to expected residual variation. The pooled residual variation is found as the average standard deviation for all data elements.

Table I. Explained variance as a percentage vs the number of components for PARAFAC models of the fluorescence data with 1 –5 components

	No. of components				
	1	2	3	4	5
Explained variance (%)	84.7	98.1	99.4	99.6	99.8
Core consistency (%)	100	100	37	31	10

The core consistency diagnostic is an approach suggested for finding the number of components to use in multi-way models such as PARAFAC [4]. A so-called Tucker3-like core array is calculated from the data and the PARAFAC loadings. The relative sum-of-squared difference between this core and a superdiagonal core of ones is called the core consistency. It is usually expressed as a percentage. A PARAFAC model can be represented as a constrained Tucker3 model where the core has been forced to a superdiagonal of ones (trilinearity) and the consistency provides a quantitative measure of how well the loadings represent variation in the data consistent with this assumption. If the core consistency is not close to 100%, the model does not give an appropriate description of the data and a lower number of components should be chosen (see Bro [4] for more details). Core consistencies for the five models are shown in Table I. A two-component model gives a core consistency of 100%. The core consistency of the three-component model of 37% indicates that this model might not be stable and hence core consistency points to two components being optimal. However, as noted above, the percentage of variation explained for these data points to

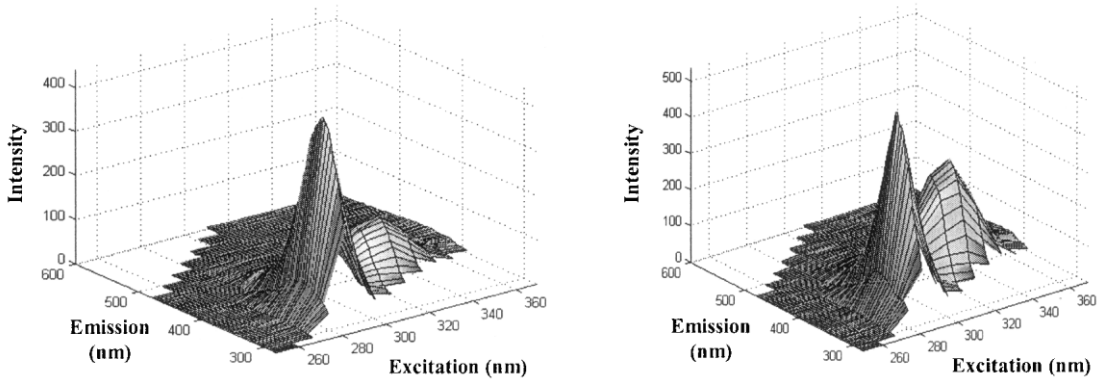

Figure 3. Examples of fluorescence excitation–emission landscapes. Emission spectra were collected from 280 to 600 nm after excitation from 250 to 370 nm. Note that triangular parts of the landscapes have been set to missing.

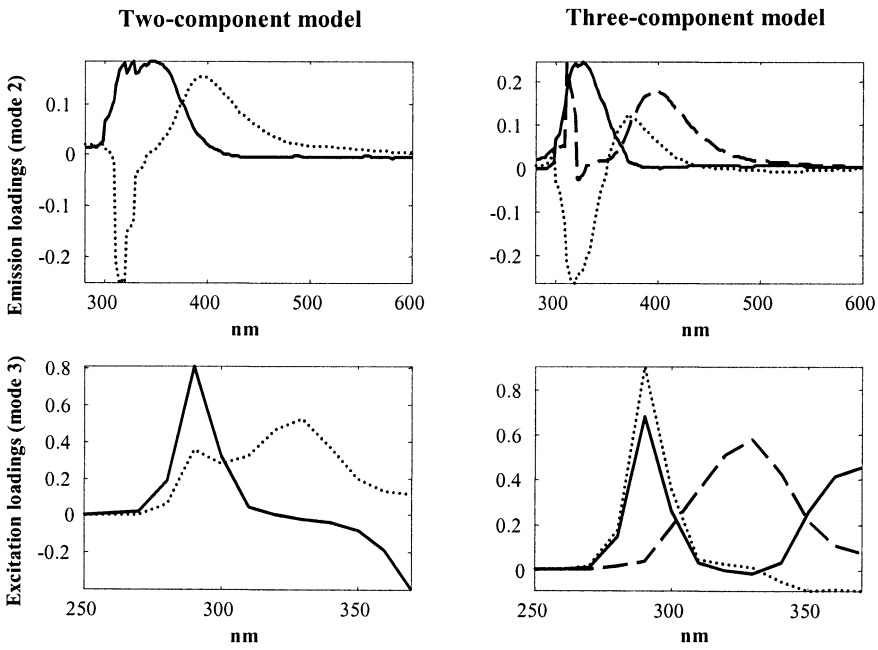

Figure 4. Emission and excitation loadings of two- and three-component PARAFAC models. The lines indicate component one (solid), component two (dotted) and component three (dashed).

three components possibly being adequate. It is not uncommon that different diagnostics point to different numbers of components, especially in this early stage of an analysis. Further elaboration will help to clear up such controversies and no final conclusions are drawn at this stage.

When fitting a model several times from random starting positions, the same solution is typically obtained for all or most models if the right number of components is chosen. When too many components are extracted, the number of local minima (different model fit values when fitting from different starting points) often increases. In the actual situation, the three-component model repeatedly converged to the same solution. This does not provide conclusive evidence, but together with the conclusions from looking at the fit values, it does indicate that three components may be feasible.

A so-called two-factor degeneracy is a situation in which two of the components are virtually identical but of opposite sign [25]. This typically occurs when too many components are extracted. Here, no degeneracy is found for the three-component solution. Although the absence of local minima and degeneracies are only to be used as very *ad hoc* diagnostics, these signs together with the fit values do indicate that three components might be an option upon further analysis.

3.1.1.2. Visual appearance of the loadings. When the fluorescence data follow a trilinear model, the correctly validated PARAFAC emission and excitation loadings are estimates of the pure analyte fluorescence spectra when the correct number of components is used. Figure 4 shows the loadings of the two- and three-component models. The emission spectra in both models have characteristics that are not consistent with the expectations. The sharp peaks around 300 nm and the large negative regions indicate that the models are not correctly identifying spectra of pure chemical components.

Probably the high and narrow peak in the estimated emissions of component three (Figure 4) is an artifact caused by a combination of the large amount of low-emission missing data (Figure 3) and the presence of small amounts of scatter remaining in the specific area. This will be elaborated on below.

3.1.1.3. Jack-knife validation of the loadings. One way to evaluate the stability of the model is by an exploratory use of the jack-knife method. Jack-knifing is a resampling method that can be used for assessing the uncertainty of the model parameter estimates such as scores and loadings [26]. Multiple models are fitted by leaving out one sample at a time. For these data, then, 105 versions of the loadings are obtained, which can be used for evaluating the model stability and for outlier detection [27]. Figure 5 shows the standard errors of the 105 estimated emissions for the three-component model. Large standard errors are obtained for component three in the wavelength area with the high and narrow peak (Figure 4). Also for component two, part of the wavelengths corresponding to areas with supposedly unreliable loadings have high standard errors. This component shows emission loadings with both a negative and a positive peak.

3.1.1.4. Explaining artifactual loadings. By jack-knifing, a quantitative measure of the uncertainty is obtained, but no explanation for the problematic loading shapes can be obtained from these results directly. The sharp low-wavelength peak is, in fact, a spurious result of the pattern

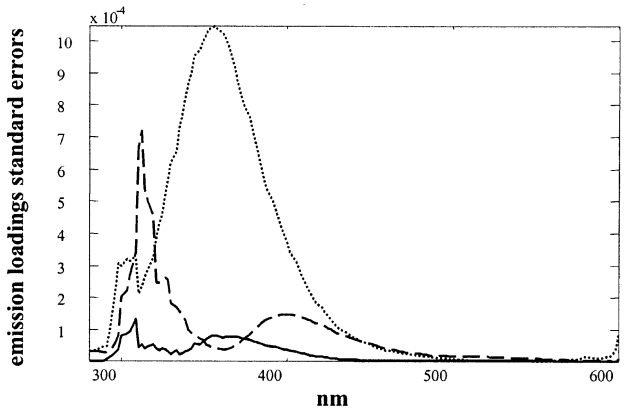

Figure 5. Standard errors of the loadings of the three-component PARAFAC model (Figure 4) obtained by jack-knife validation. Jack-knife is performed by leaving one sample out at a time. The lines indicate component one (solid), component two (dotted) and component three (dashed).

of missing values. In order to see why the peak appears, the structures described by components one and two of the three-component model are subtracted from the original data. Thus, only noise and the structure described by the third component remains in these residuals and hence represents the variation that component three is seeking to explain. Visualizing this part of the data can help in understanding why the estimated emission profile is peculiar. Figure 6(a) shows an example of these residuals illustrating the peak caused by a chemical phenomenon corresponding to the broad peak of component three. The high and narrow peak around emissions at 300 nm is not visually detectable. In addition, the outer product of the emission and excitation loadings of component three is given (Figure 6(b)). The outer product provides a full landscape but if the missing elements in the data are set to missing in the component three landscape, Figure 6(c) is obtained. The high and narrow peak in the emission loadings causes a narrow peak in the full landscape positioned in a part where there are no measurements. The peak arises because it is describing a small remaining scatter peak in the original landscape in the low excitation area (circle in Figure 6(a)). Owing to the pattern of missing values, the size of this small peak relative to the large chemical peak is largely *unrelated*. Thus, the magnitude of the two peaks in component three cannot be compared directly. The apparent large sharp peak is an artifact that appears owing to the combined effect of the small amount of Rayleigh scatter left and the missing data. As such the peak is correct but its relatively high magnitude is disturbing from an exploratory point of view. A similar explanation of the inferior appearance of the loadings of component two can be given even though the appearance of component two differs from that of component three.

The above indicates that more data elements need to be set to missing because there are still parts influenced by scatter. However, setting more elements to missing would mean that parts of the interesting chemical variation are also eliminated, leading to a lower information level, which is not feasible. There are several alternative ways of dealing with this problem [4,24,28]. Below it will be shown how the application of constraints on the parameters can be helpful to this end. It is emphasized, however, that the apparently artifactual peaks are not incorrect numerically but merely annoying in visual interpretation of the parameters. Before applying constraints an initial look at the currently obtained score values is performed to check for extreme outliers.

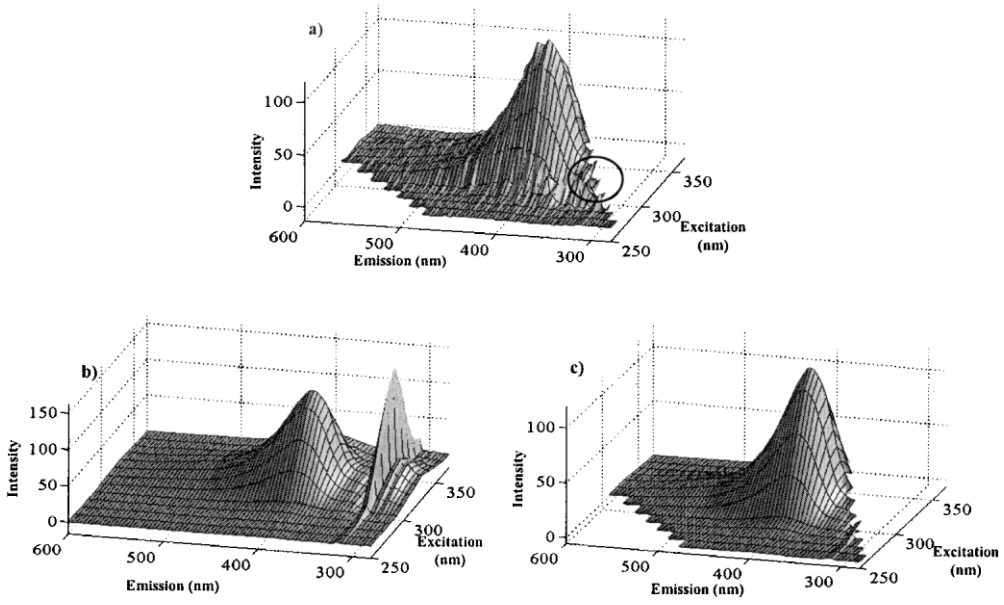

Figure 6. (a) Example of an excitation–emission matrix after removing components one and two obtained from the three-component PARAFAC model; (b) outer products of emission and excitation loadings of component three of the three-component PARAFAC model; (c) as in (b) with the wavelength areas corresponding to missing values in the original data set to missing.

3.1.1.5. Initial evaluation of score values. Extreme score values in the sample mode indicate possible outliers. Figure 7 shows scatter plots of the scores obtained from the three-component PARAFAC model (loadings are shown in Figure 4). All scores are of similar magnitude and no extreme outliers are indicated on the basis of the score values. However, there may be more subtle outliers, which cannot be identified only by studying the score values. More dedicated diagnostics will be needed for identification of such outliers but is postponed as the immediate check for gross outliers suffices at this stage of the analysis.

The score plot shows an unexpected partly collinear behavior of the scores for two of the components. While this may be due to chemical properties of the system, it is disturbing that it apparently only occurs for a (major) part of the data. If this is reflecting a real underlying phenomenon, then likely an unfortunate sampling has been used. However, comparing with Figure 4, the corresponding emission spectra seem to be partly confounded having a similarly shaped low-emission peak. Most likely these two components are hence partly describing the same underlying phenomena, possibly caused by scattering. In the actual model described later, the same phenomenon is not observed, hinting at the appropriateness of the constraints suggested next.

3.1.1.6. Applying constraints. Constraining the parameters of the PARAFAC model can be helpful in terms of interpretability, curve resolution and stability of the solution. It may be argued that constraints should not be necessary if the data behave according to the model. However, as exemplified above, minor details in the data can impose large changes in the estimated parameters that disturb proper interpretation. Constraints can help to remedy such problems. Caution is needed, however, to make sure that the constraints are not otherwise disturbing the appearance of important phenomena.

The loadings shown in Figure 4 are unimodal apart from the unstable part. It is expected that that the real spectra are non-negative and thus, constraining with both non-negativity and unimodality could possibly help in modeling the problematic part of the fluorescence landscapes. Various combinations of non-negativity and unimodality constraints in the three modes were tried and evaluated by explained variance, core consistency and visual appearance of the loadings. It was found that applying non-negativity in the sample mode and both unimodality and non-negativity in the two other modes (excitation and emission) performed well. The loadings thus obtained for two- and three-component models are illustrated in Figure 8. The visual appearance of the loadings indicates that the constrained models give a more appropriate description of the underlying spectral phenomena than the unconstrained models, not being excessively influenced by the minor remaining scatter variation. The second excitation component of the two-component constrained model has a shoulder indicating that the data contain more than two components.

In order to validate the appropriateness of constraints, the changes caused by these must be explainable. For example, for non-negative constraints the loadings should show peaks at reasonable positions compared to the raw data but with negative parts removed. The changes can be seen by comparing Figure 8 with Figure 4. The loadings have been forced to be unimodal whereby inferior peaks caused by scatter and missing values have been removed. The danger of applying constraints is that the parameters are forced to correspond to the *a priori* knowledge without necessarily being more adequate. However, by comparing the solutions carefully, the risk of misleading models can easily be avoided. In this case, the spectral profiles are similar to the unconstrained profiles except that understood low-variance artifacts are removed.

A core consistency of 59% for the three-component model shows that systematic variation is present in all three factors. Compared with the core consistency of the three-component

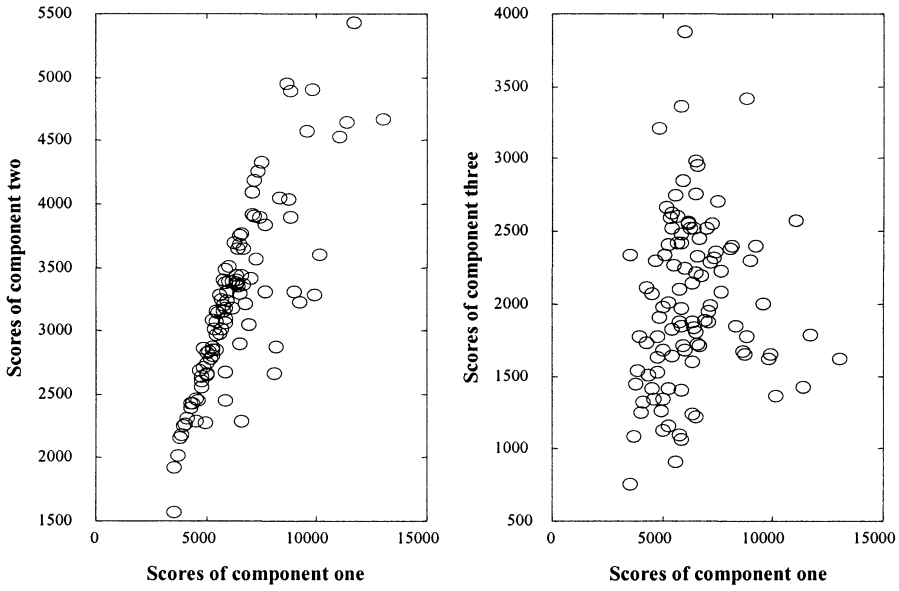

Figure 7. Scatter plot of the score values obtained for the three-component PARAFAC model.

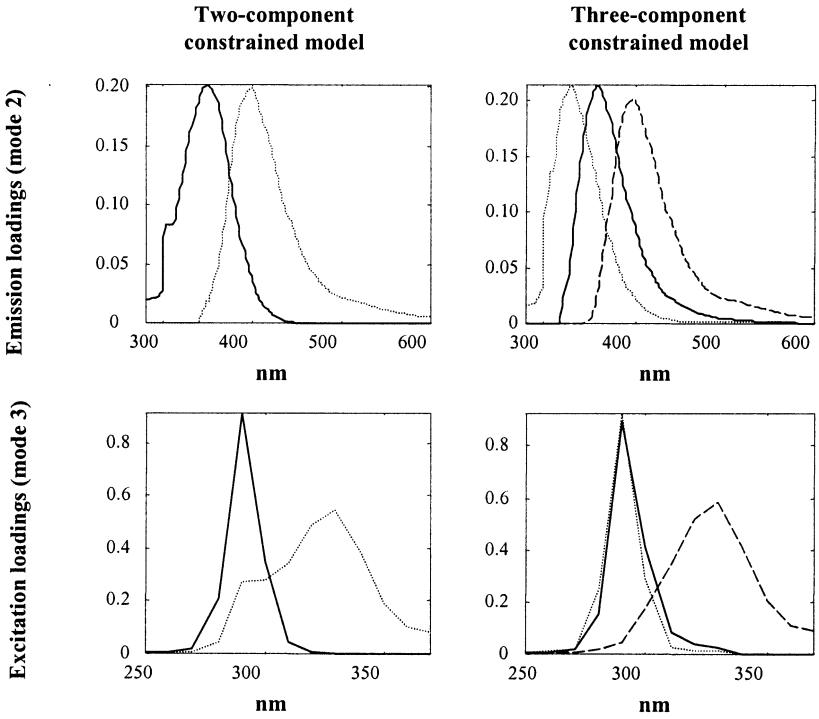

Figure 8. Emission and excitation loadings of two- and three-component PARAFAC models constrained with non-negativity in mode one and non-negativity and unimodality in modes two and three. The lines indicate component one (solid), component two (dotted) and component three (dashed).

unconstrained model of 37% (Table I), this shows that applying constraints increases the model validity although the core consistency is still lower than hoped for. This, probably, reflects that the three components are somewhat difficult to estimate. The explained variance increases from 97.6 to 99.1 on increasing the number of components from two to three. The last value should be compared with the explained variance of the three-component unconstrained model of 99.4% (Table I). The fit of a constrained model will be lower than that for an unconstrained model by definition, but the similarity of fits shows that the constrained model is mainly filtering off insignificant noise and not systematic variation. Hence, the constraints seem valid also from this perspective.

From the discussion above, the non-negativity and unimodality constrained three-component model is found to give a valid description of the excitation–emission data.

3.1.2. *Data with known fluorophores*

Since the data set contains four analytical compounds, it is expected that four PARAFAC components are appropriate and the reliability of four components will be verified below. Initial modeling indicates the presence of four or five components as evaluated from the explained variance and the number of iterations (Figure 9). When too many components are included, the number of iterations will typically increase dramatically as seen for the six-component model. However, the number of iterations can only be used as an indication since, e.g., highly correlated components will often require many iterations and a model with too many factors can sometimes be easy to fit. Furthermore, an unlucky initialization may lead to many iterations even though the model is perfectly sound. Still, using *ad hoc* measures such as the number of iterations, number of local minima, etc., is useful in practice.

The five-component model indicates that the low excitations are very noisy. This is seen in Figure 10, which shows

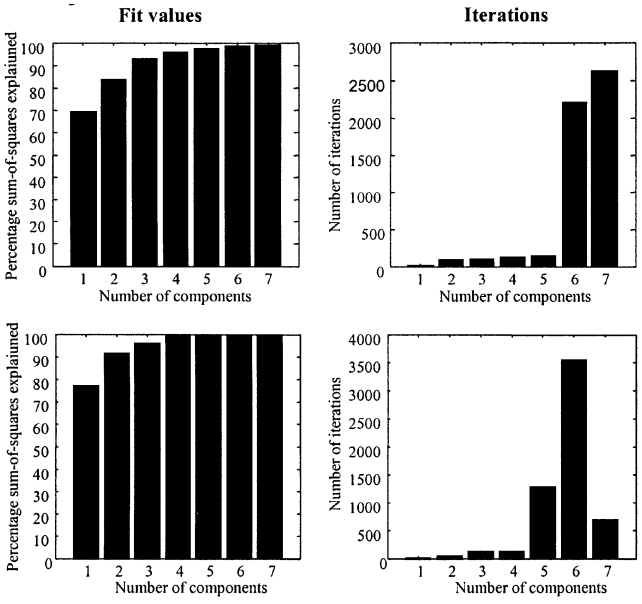

Figure 9. Fit values and number of iterations as a function of the number of components, all data included (top) and low excitation and emission removed (bottom).

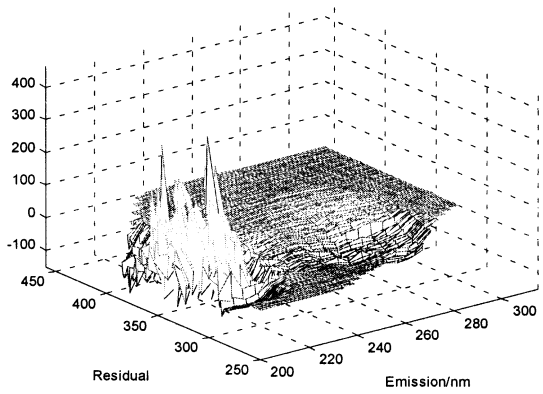

Figure 10. Residuals of sample one from a five-component PARAFAC model.

an example of the residuals of sample one. The reason for this noise is to be found in the properties of the instrument. In order to reduce the effect of the noise, excitations below 230 nm were excluded, as were also emissions below 260 nm.

After excluding the noisy part it becomes clear that four components provide a valid PARAFAC model. The four-component model explains approximately 100% of the variation in the data and the number of iterations increases considerably when fitting more components. The reliability is further verified by the excitation and emission loadings, which have shapes resembling pure spectra (Figure 11).

3.2. Finding outliers

3.2.1. Fish data

The three-component model constrained with non-negativity in the first mode and non-negativity and unimodality in both the second and third modes is chosen for further detailed analysis and validation. After the initial analysis, the possible presence of more subtle outliers should be monitored for and possibly removed. Here, jack-knife resampling and an investigation of the residuals is used for the identification of outliers.

An identity match plot obtained from the jack-knife procedure was suggested by Riu and Bro [27] for identification of outliers. In the plot, the predicted score of the sample left out is plotted against the score obtained by the overall model. Potential outliers will be placed away from the ideal identity line, showing that the quantitative information on the samples differs markedly whether or not the sample is included in the analysis. The plot is made for each of the three components separately (Figure 12, top plots) showing that sample number 42 is a clear outlier. Its score values differ markedly depending on whether it is included in the model or not. Hence its spectral characteristics are not covered by those of the remaining samples which almost by definition makes it an outlier. The fact that sample 42 is an outlier is supported by the fluorescence landscape and the residuals of this sample. The bottom-left plot in Figure 12 shows the fluorescence landscape. One of the peaks contains elements with an intensity larger than what can be measured with the given instrument settings (out of range). These elements are given as missing values in the data set. Even though this peak has a similar shape to the same peak in all the other samples, it is possible that the larger amount of missing values makes the modeling of the sample difficult or uncertain. This is supported by the systematic variation left in the residuals shown in the plot to the right. Thus, there is significant structure in the fluorescence landscape of sample 42, which is not modeled.

Other diagnostics than the identity match plot can be used for detecting outliers by the jack-knife technique. For example, an outlying sample may have a large uncertainty in the score values as estimated from the resampled models. Furthermore, an indication of an outlier could be a sample where the estimated loadings obtained when leaving out this sample differ from the corresponding loadings obtained from all samples. These approaches were also applied here, but did not indicate additional outliers.

All samples should have low residuals compared with the measured spectra. Furthermore, residuals should ideally be randomly distributed, meaning that the remaining unexplained variations would only be caused by random noise. Sometimes, however, systematic variation can remain in the residuals, reflecting unmodeled scatter effects of chemical interactions. The model may still be valid, as long the estimated parameters can be properly validated.

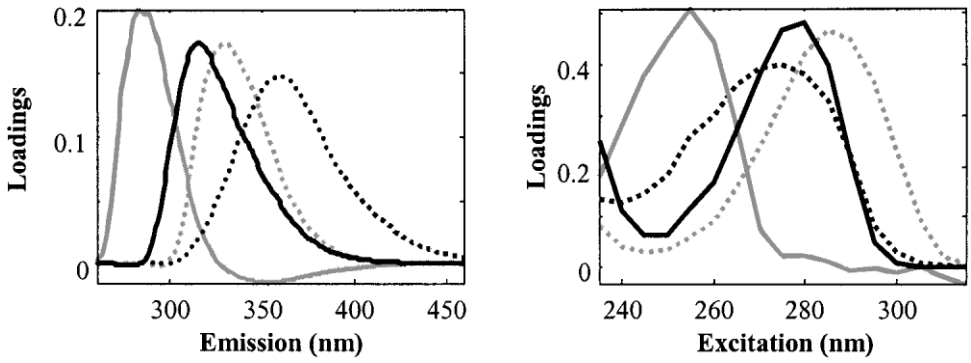

Figure 11. A four-component PARAFAC model on all calibration samples with low excitations removed, emission mode loadings (left) and excitation mode loadings (right). The lines indicate component one (black solid), component two (black dotted), component three (gray solid) and component four (gray dotted).

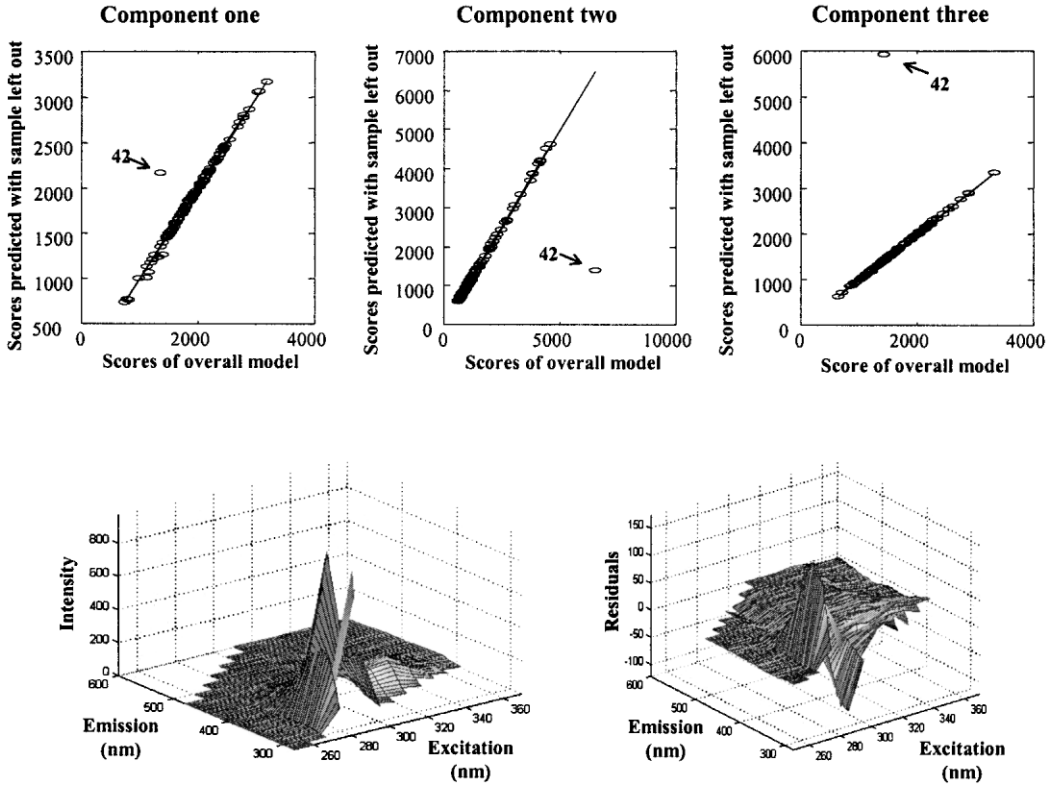

Figure 12. Top plots: identity match plots of the scores from the constrained three-component PARAFAC model. Bottom-left plot: fluorescence excitation–matrix of sample 42. Bottom-right plot: residuals of sample 42 for a three-component PARAFAC model.

A constrained three-component PARAFAC model with sample 42 left out shows that three other samples may be considered outliers as judged from their residuals. The top-left plot in Figure 13 shows the sum of squared residuals of each sample. Fairly large values are observed for the samples 14, 37 and 82, which also have systematically distributed

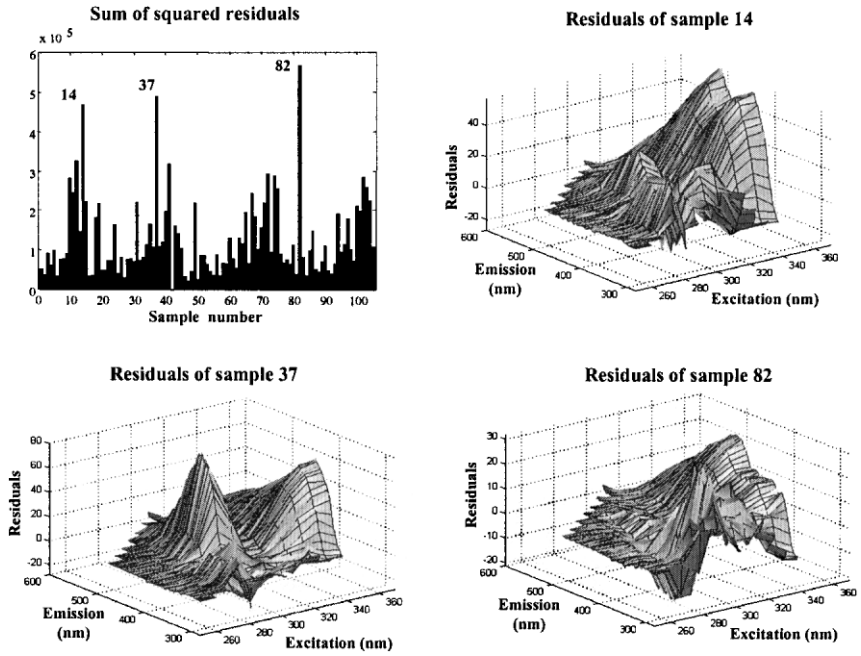

Figure 13. Plots illustrating possible outliers in a constrained three-component PARAFAC model where sample 42 is removed. Sum of squared residuals for all samples and distribution of residuals for samples 14, 37 and 82 are shown.

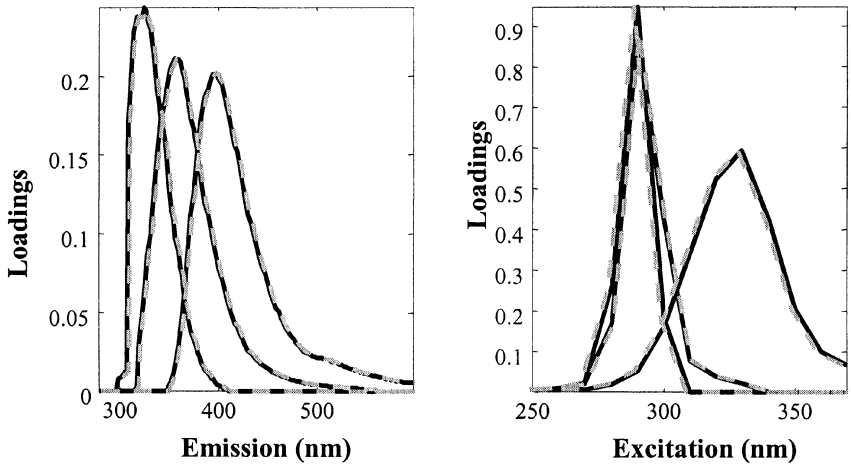

Figure 14. Emission (left) and excitation (right) loadings for constrained three-component PARAFAC models with sample 42 left out (black solid) and samples 14, 37, 42 and 82 left out (gray dashed).

residuals (Figure 13). Therefore, new models are evaluated with those samples removed.

An explained variation of 99.1% and a core consistency of around 50% are obtained irrespective of the removal of outliers or not. Figure 14 shows the loadings of PARAFAC models with sample 42 left out and with the samples 14, 37, 42 and 82 left out. The loadings of the two models are similar, indicating that the three samples (14, 37 and 82) are of similar type as the remaining and hence help in supporting the model. Therefore, these three samples are kept in the model.

3.2.2. *Data with known fluorophores*

Another way to illustrate the presence of outliers is by a residual and influence analysis. This is illustrated for the four-component PARAFAC model made on the fluorescence landscapes of the four analytes. Figure 15 shows that no samples have very large residuals but samples 2, 3 and 4 seem to have somewhat large leverages. As for the other data set, the influence of the high-leverage samples on the model parameter estimates should be evaluated. It was found that the loadings did not change on removing the possible outliers and the samples should, therefore, be kept in the model.

Samples 2, 3, and 4 have high concentrations of either hydroquinone, tryptophan or DOPA. Hence the high residuals may be due the high concentrations leading to slightly changed lineshapes of the spectra, e.g. due to inner-filter effects.

3.3. Split-half validations

In order finally to validate the appropriateness of the models built on data with the chosen outliers removed, split-half analysis [19] is applied. In split-half analysis, different subsets of data are analyzed independently. Owing to the uniqueness of the PARAFAC model, the same spectral loadings will be obtained from different samples if the samples reflect the same fluorophores, when the correct number of components is chosen and enough data are available in each subset.

3.3.1. *Fish data*

A model constrained with non-negativity in the first mode and unimodality together with non-negativity in the second and third modes is used. In addition, one sample (42) has been excluded as an outlier. The samples are divided according to storage temperature. Thereby all variations in the fluorescence spectra will be found in both data sets. The loadings obtained from two split-half data sets are illustrated in Figure 16. The differences between the two data sets can hardly be discerned and the chosen model, therefore, seems to give a reliable and adequate description of underlying fundamental phenomena.

3.3.2. *Data with known fluorophores*

The split-half analysis was performed by dividing the samples into two subsets where both subsets contain information on all four fluorophores. The splitting was

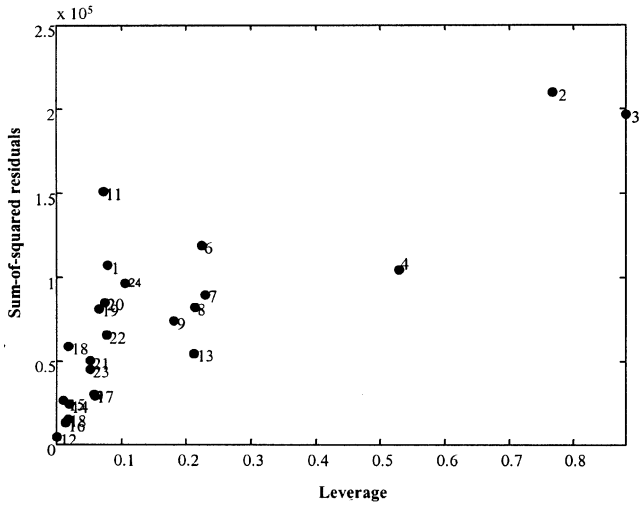

Figure 15. Influence plot of four-component PARAFAC model. The sum-of-squared residuals summed within the same mode are plotted against the leverage of the first mode components. Each sample is labeled by number.

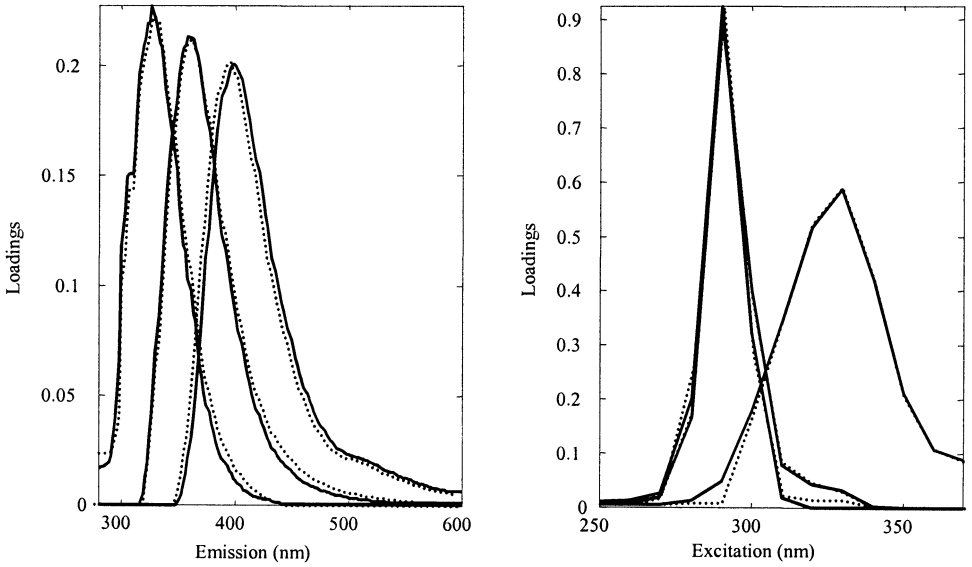

Figure 16. Results from a split-half analysis. The split-half is performed by dividing the samples into groups depending on the storage temperature. Solid lines show samples stored at −30 °C and dotted lines show samples stored at −20 °C.

made in two ways, giving four different subsets that were pairwise independent. The graphical representation in Figure 17 illustrates the reliability of four components.

3.4. Interpretation

3.4.1. Interpretation of scores and loadings of the fish data

The estimated excitation spectra have maxima at 290 and 330 nm (Figure 8). This corresponds to the peaks in the raw fluorescence landscapes (Figure 3). Components one and two have the same position of the excitation maximum but different positions of the emission maxima that are found at 360 and 330 nm for the two components, respectively. In fact, the excitation loadings of those two components are almost identical. The reason for the similarity of these loadings can be that they reflect the same fluorophores but with different substitutions, one or both are bounded to another molecule or that they are identical fluorophores appearing in slightly different electronic environments. This leads to slight differences in spectral characteristics. This was also illustrated by Ross and Leurgans [5], who showed that the estimated excitation spectrum of tyrosine dissolved in water was almost similar to the estimated excitation spectrum of tyrosine bound to phosphate. However, the minor differences in the loadings were sufficient for estimating them separately. The possibility of separating fluorophores with similar excitation maxima shows the value of using PARAFAC for curve resolution and for describing the underlying spectral phenomena. The fluorophore described by component three has excitation maximum around 330 nm and emission maximum around 400 nm.

Investigating press juices and aqueous extracts of fish muscles, a fluorophore associated with dissolved muscle proteins was earlier shown to have excitation/emission maxima at 292/340 nm [29]. Thus, the two fluorophores obtained in the present study with excitation maxima around 290 nm might be related to the presence of muscle proteins. Tryptophan, tyrosine and phenylalanine are the amino acids responsible for the fluorescence of proteins.

Adding tryptophan in various concentrations to the cod extracts and comparing the thus obtained fluorescence with the fluorescence measured on pure extracts indicates the presence of tryptophan. It is found that loadings of a PARAFAC model made on fluorescence spectra of cod

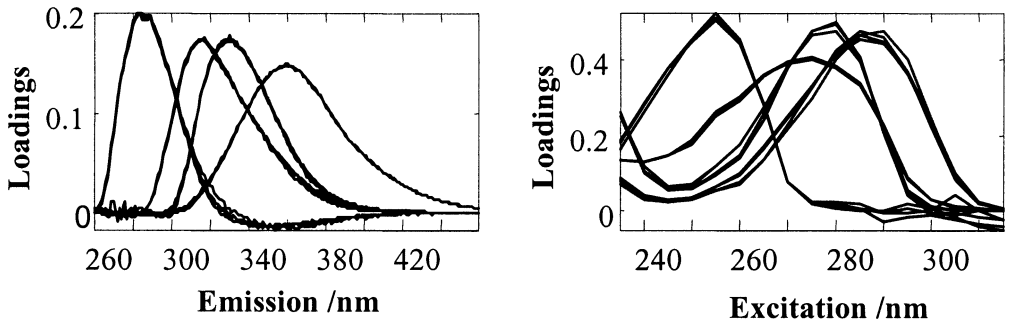

Figure 17. Results from split-half analysis, emission mode loadings (left) and excitation mode loadings (right).

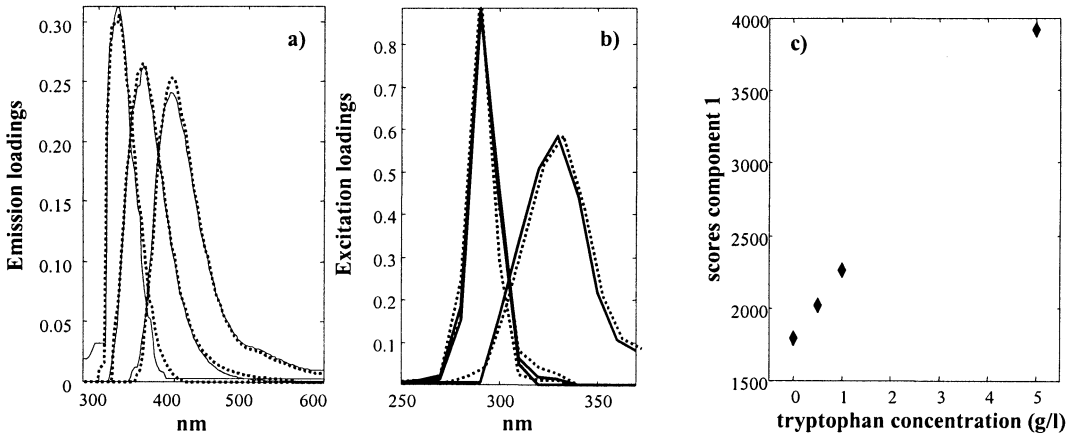

Figure 18. (a) Emission and (b) excitation loadings for a three-component PARAFAC model made on fluorescence spectra of cod extracts added with tryptophan (solid) and excitation and emission loadings for a three-component PARAFAC model made on fluorescence spectra of the pure cod extracts (dotted). (c) Relation between the score values of component 1 and the concentration of added tryptophan.

extracts with added tryptophan are similar to the loadings of the PARAFAC model made on fluorescence spectra of the pure cod extracts (Figure 18(a) and (b)). The presence of tryptophan in the cod extracts is further substantiated by a linear relation between the score values of component one and the concentration of tryptophan added to the extracts (Figure 18(c)). The fluorophore of component two, which has the same excitation spectrum as the tryptophan component but a different emission spectrum, might also be tryptophan with a substituent or bound to another molecule. There is no linear relation between the scores of this component and the tryptophan concentration.

The scores of the model are estimates of the relative concentrations of the fluorophores identified by the loadings and are therefore measures of the amount of the fluorophores present. For component two and perhaps also component one, there are weak correlations to the chill storage time (Figure 19). These relations could not be seen when comparing visually the intensities of the two peaks with the chill storage time. The change in fluorescence intensity with storage time has been shown in other studies [30,31]. However, the present study illustrates an explorative way of identifying chemically meaningful quality parameters that can possibly be monitored industrially.

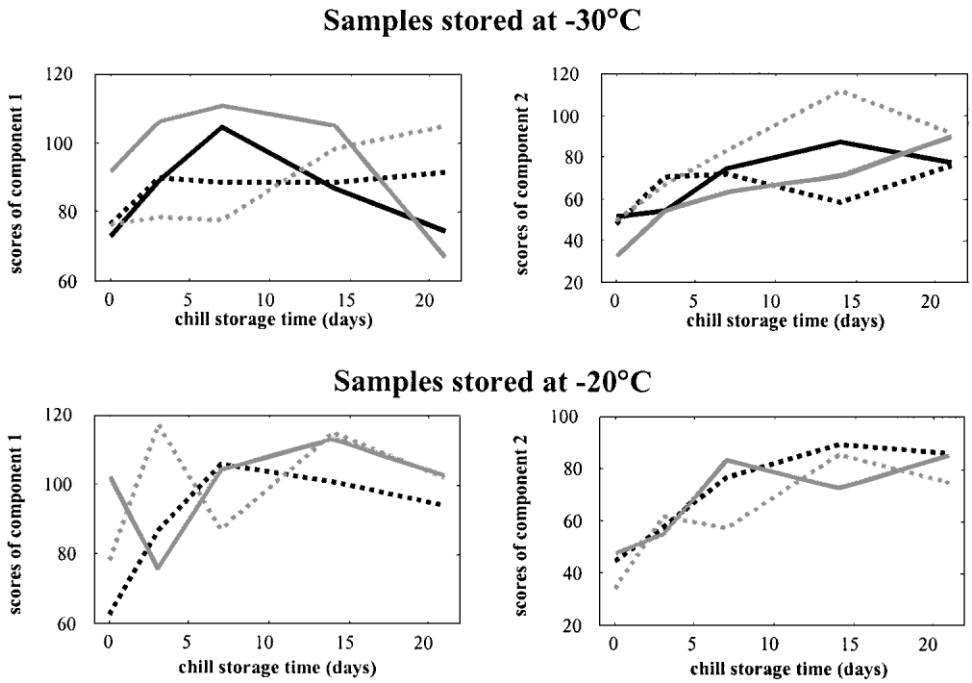

Figure 19. Relation between chill storage time and scores of the constrained three-component PARAFAC model. Scores are corrected for the different weights of fish muscle used for making the extracts. The lines indicate different freeze storage time: 3 months (solid black), 6 months (dotted black), 9 months (solid gray) and 12 months (dotted gray).

Another study using the same fish material showed a correlation between the chill storage time and drip loss of water and between chill storage time and the sensory parameter juiciness [32]. When proteins degrade, smaller peptides are produced. This reduces the ability of the muscle to hold water and results in an increased drip loss related to the development of smaller protein fragments. Thus, the increase in the score values may reflect an increase in the content of small peptides produced during chill storage. This is also verified by the positions of peak maxima in the excitation and emission loadings of components one and two.

No relation was found between the score values and the freeze storage temperature or between the score values and the freeze storage time. This suggests that these two storage conditions do not have an effect on the development or disappearance of fluorescent chemical compounds in the fish muscle extracts.

Fluorescence correlated with lipid oxidation was found to have excitation maximum at 360–370 nm [33,34]. In the present study, fluorescence with excitation higher than 370 nm was not measured because no emission was obtained for excitation higher than 370 nm. Therefore, lipid oxidation is probably not detected. NADH does have an important impact on autofluorescence originating from fresh fish muscle [35], but it has been found that the NADH content of fish muscle has almost disappeared after freezing and thawing [29] and probably NADH will have no or only very little influence on the fluorescence spectra obtained in this study. However, component three with excitation/emission maxima around 330/400 nm may conform to the excitation and emission maxima of NADH that are found at 340 and 450 nm, respectively [35]. The difference in peak maxima between the component obtained here by PARAFAC and the value for NADH given in the literature may be an effect of the sample matrix in that the exact position of the peaks depends on the sample composition and the measurement conditions. However, if component three describes NADH, an effect of the chill storage time is expected, which was not seen. Nevertheless, the relation between fluorescence of fish muscle and NADH or lipid oxidation should be investigated more thoroughly because the NADH content decreases and lipid oxidation develops during storage. Therefore, prediction of these parameters by fluorescence spectroscopy could be an indicator of fish freshness.

It is not possible to identify fully the underlying spectral phenomena that PARAFAC found to be contributing to the fluorescence of aqueous cod extracts. In order to do so, several approaches can be feasible. Chromatographic separation before fluorescence measurements, as was shown by Baunsgaard *et al.* [7], may improve the identification of the fluorophores. In addition, specific peptide sequences can be separated by capillary electrophoresis. This may be used for identifying the component with excitation maximum at 290 nm, which was not tryptophan. Furthermore, standard addition can be used for verifying the presence of certain fluorophores as shown for tryptophan.

3.4.2. *Using the model on new data*

Below it is shown how the parameters of the PARAFAC model can be used on new fluorescence spectroscopic data, e.g. for the determination of analyte concentrations. In the data set with the four fluorophores, the concentration of the four analytes in each sample is known. Therefore, it is possible to make a calibration model from the relation between the score values and concentration of one of the analytes. If the PARAFAC model is made only on a part of the samples, the scores of the samples left out can be estimated by fitting a new PARAFAC model with the spectral loadings fixed to those of the original solution. From the estimated scores, the concentration of the analyte can be estimated from the calibration model.

The loadings of component four resemble the pure spectra of tryptophan. Therefore, score values of this component and the corresponding analyte concentrations are used for making a univariate calibration model for tryptophan. Three samples were not used in building the PARAFAC model and the score values of these samples and also the analyte concentration can be estimated from the model. Figure 20 shows the tryptophan concentration predicted from the calibration model versus the known concentrations, illustrating that the calibration model performs well. The concentration of tryptophan in the samples left out (test samples) is obtained from the estimated score values and the regression coefficient of the calibration model. In the predicted versus measured plot it is seen that sample 5 is not predicted well, whereas good predictions are obtained for samples 10 and 15. A high residual and large leverage were obtained in the estimation of the score values of sample 5. This reveals that it is an extreme sample and also explains why the tryptophan concentration is not predicted well.

4. CONCLUSION

This paper has given a presentation of the steps involved in finding an optimal PARAFAC model. The focus has been on

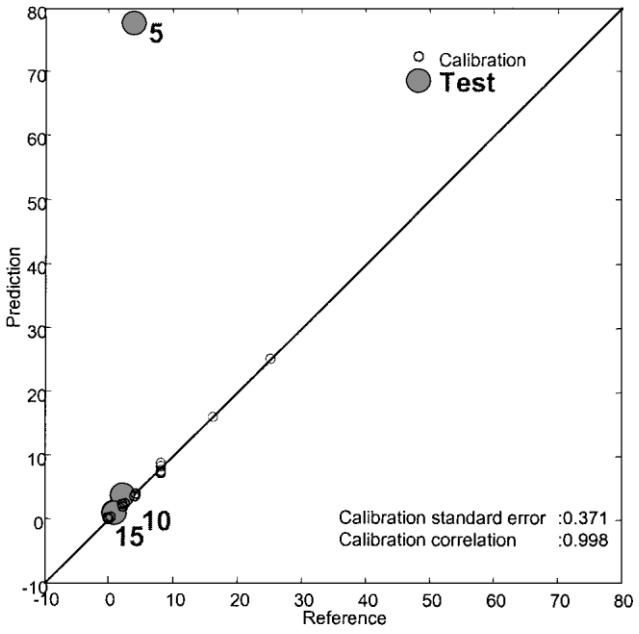

Figure 20. Predicted versus reference concentration of tryptophan. Test samples are shown with solid circles.

the practical application of PARAFAC modeling of complex data. Problems with, e.g., scattering and missing values have been given special attention. It has been shown when and how to apply constraints, identify outliers and validate the model. Finally, model interpretation and the possibility of using the results of the PARAFAC model on new samples are illustrated.

Acknowledgements

The authors acknowledge financial support through LMC (Center for Advanced Food Studies) and AQM (Advanced Quality Monitoring), supported by the Ministries of Research and Industry. R. Bro is grateful for support from EU Project GRD1-10337, NWAYQUAL. Niels Bøknæs is gratefully acknowledged for providing the materials.

REFERENCES

1. Harshman RA. Foundations on the PARAFAC procedure: model and conditions for an "explanatory" multimode factors analysis. *UCLA Working Pap. Phonetics* 1970; **16**: 1–84.
2. Leurgans S and Ross RT. Multilinear models: applications in spectroscopy. *Statist. Sci.* 1992; **7**: 289–319.
3. Kroonenberg PM. Three-mode component models. A survey of the literature. *Statist. Appl.* 1992; **4**: 619–633.
4. Bro R. *Multi-way analysis in the food industry, theory algorithms and applications*. Doctoral dissertation, University of Amsterdam, 1998.
5. Ross RT and Leurgans S. Component resolution using multilinear models. *Methods Enzymol.* 1995; **246**: 679–700.
6. Ross RT, Lee C-H, Davis CM, Ezzeddine BM, Fayyad EA and Leurgans SE. Resolution of fluorescence spectra of plant-pigment complexes using trilinear models. *Biochim. Biophys. Acta* 1991; **1056**: 317–320.
7. Baunsgaard D, Andersson CA, Arndal A and Munck L. Multi-way chemometrics for mathematical separation of fluorescent colorants and colour precursors from spectrofluorimetry of beet sugar and beet sugar thick juice as validated by HPLC analysis. *Food Chem.* 2000; **70**: 113–121.
8. Bro R. Exploratory study of sugar production using fluorescence spectroscopy and multi-way analysis. *Chemom. Intell. Lab. Syst.* 1999; **46**: 133–147.
9. Jiji RD, Andersson GG and Booksh KS. Application of PARAFAC for calibration with excitation–emission matrix fluorescence spectra of three classes of environmental pollutants. *J. Chemom.* 2000; **14**: 170–185.
10. Jiji RD, Cooper GA and Booksh KS. Excitation–emission matrix fluorescence based determination of carbamate pesticides and polycyclic aromatic hydrocarbons. *Anal. Chim. Acta* 1999; **397**: 61–72.
11. Moberg L, Robertsson G and Karlberg B. Spectrofluorimetric determination of chlorophylls and pheopigments using parallel factor analysis. *Talanta* 2001; **54**: 161–170.
12. Pedersen DK, Munck L and Engelsen SB. Screening for dioxin in fish oil by PARAFAC and N-PLSR analysis of fluorescence landscapes. *J. Chemom.* 2002; **16**: 451–460.
13. Harshman RA and Lundy ME. PARAFAC: parallel factor analysis. *Comput. Statist. Data Anal.* 1994; **18**: 39–72.
14. Bro R. Parafac: tutorial and applications. *Chemom. Intell. Lab. Syst.* 1997; **38**: 149–171.
15. Ewing GW. *Instrumental Methods of Chemical Analysis*. McGraw-Hill: Singapore, 1985.
16. Nørgaard L. Direct standardisation in multi-wavelength fluorescence spectroscopy. *Cemom. Intell. Lab. Syst.* 1995; **29**: 283–293.
17. Baunsgaard D. *Factors affecting 3-way modelling (PARAFAC) of fluorescence landscapes*. Thesis. The Royal Veterinary and Agricultural University: Fredericksberg, 1999.
18. Sidiropoulos ND and Bro R. On the uniqueness of multilinear decomposition of N-way arrays. *J. Chemom.* 2000; **4**: 229–239.
19. Harshman RA and de Sarbo WS. An application of PARAFAC to a small sample problem, demonstrating preprocessing, orthogonality constraints, and split-half diagnostic techniques. In *Research Methods for Multimode Data Analysis*, Law HG, Snyder CW, Hattie JA, McDonald RP (eds). Praeger: New York, 1984; 602–642.
20. Heimdal H, Bro R, Larsen LM and Poll L. Prediction of polyphenol oxidase activity in model solutions containing various combinations of chlorogenic acid, (−)-epicatechin, O_2, CO_2, temperature, and pH by multiway data analysis. *J. Agric. Food Chem.* 1997; **45**: 2399–2406.
21. Bro R and Heimdal H. Enzymatic browning of vegetables. Calibration and analysis of variance by multi-way methods. *Chemom. Intell. Lab. Syst.* 1996; **34**: 85–102.
22. Jiji RD and Booksh KS. Mitigation of Rayleigh and Raman spectral interferences in multi-way calibration of excitation–emission matrix fluorescence data. *Anal. Chem.* 2000; **72**: 718–725.
23. Wentzell P, Nair SS and Guy RD. Three-way analysis of fluorescence spectra of polycyclic aromatic hydrocarbons with quenching by nitromethane. *Anal. Chem.* 2001; **73**: 1408–1415.
24. Bro R, Sidiropoulos ND and Smilde AK. Maximum likelihood fitting using ordinary least squares algorithms. *J. Chemom.* 2002; **16**: 387–400.
25. Kruskal JB, Harshman RA and Lundy ME. How 3-MFA data can cause degenerate PARAFAC solutions, among other relationships. In *Multiway Data Analysis*, Coppi R, Bolasco S (eds). Elsevier: Amsterdam, 1989; 115–122.
26. Efron B and Tibshirani RJ. *An Introduction to the Bootstrap*. Chapman & Hall: New York, 1993.
27. Riu J and Bro R. Jack-knife for estimation of standard errors and outlier detection in parafac models. *Chemom. Intel. Lab. Syst.* 2002; **65**: 35–49.
28. Bro R and Sidiropoulos ND. Least squares algorithms under unimodality and non-negativity constraints. *J. Chemom.* 1998; **12**: 223–247.
29. Davis HK. Fluorescence of fish muscle: description and measurements of changes occurring during frozen storage. *J. Sci. Food Agric.* 1982; **33**: 1138–1142.
30. Aubourg SP, Medina I and Gallardo JM. Quality assessment of blue whiting (*Micromesistus poutassou*) during chilled storage by monitoring lipid damages. *J. Agric. Food Chem.* 1998; **46**: 3662–3666.
31. Andersen CM and Wold JP. Fluorescence from muscle and connective tissue from cod and salmon. *J. Agric. Food Chem.* 2003; **51**: 470–476.
32. Bøknæs N, Jensen KN, Guldager HS, Østerberg C, Nielsen J and Dalgaard P. Thawed chilled Barents sea cod fillets in modified atmosphere packaging –application of multivariate data analysis to select key parameters in good manufacturing practice. *Lebensm. Wiss. Technol.* 2002; **35**: 436–443.
33. Undeland I, Ekstrand B and Lingert H. Lipid oxidation in herring (*Clupea harengus*) light muscle, dark muscle, and skin, stored separately or as intact fillets. *J. Am Oil Chem. Soc.* 1998; **75**: 581–590.
34. Hasegawa K, Endo Y and Fujimoto K. Oxidative deterioration in dried fish model systems assessed by solid sample fluorescence spectrophotometry. *J. Food Sci.* 1992; **57**: 1123–1126.
35. Munck L. *Principles of Fluorescence Analysis in Foods*. Longman: Harlow, 1989.